Thermal Effects on Single - Lap, Single - Bolt, Hybrid Metal – Composite Joint Stiffness

Calin-Dumitru COMAN*,[1], George PELIN[1]

*Corresponding Author
[1]INCAS – National Institute for Aerospace Research "Elie Carafoli",
B-dul Iuliu Maniu 220, Bucharest 061126, Romania,
coman.calin@incas.ro*, pelin.george@incas.ro

DOI: 10.13111/2066-8201.2018.10.3.7

Received: 04 May 2018/ Accepted: 24 July 2018/ Published: September 2018

6th International Workshop on Numerical Modelling in Aerospace Sciences, NMAS 2018,
16 - 17 May 2018, Bucharest, Romania, (held at INCAS, B-dul Iuliu Maniu 220, sector 6)
Section 3 – Modelling of structural problems in aerospace airframes

Abstract: *A three-dimensional finite element model has been developed to study the temperature effects on stiffness in linear-elastic range of the bolted metal-composite joints. In this study a quasi - symmetric lay - up for CFRP / vinyl ester epoxy laminate is used in conjunction with aluminum alloy (AA 7075 T6), having different thermal expansion coefficients. This generates an uneven load - deformation characteristics and three - dimensional stress field around the hole in single - lap single - bolt joints. The finite element model (FEM) was developed in commercial software PATRAN and the analysis including geometric and full nonlinearity frictional based contact has been performed using NASTRAN SOL 400 solver. The numerical model was calibrated using comparisons of the experimental measurements for surface strains and axial stiffness. The ability of the model to capture the three - dimensional effects such as secondary bending and through - thickness variation of stresses and strains in the presence of temperature variations is highlighted. The numerical and experimental results concluded that the thermal expansion material properties have a strong effect on the stiffness and linear behavior of the single - lap, single - bolt hybrid metal - composite joints.*

Key Works*: Composites, Bolted Joints, Thermal Expansion, Joint Stiffness*

1. INTRODUCTION

The aerospace industry became the most common application field for fiber-reinforced polymer matrix composites (PMCs) due to their lightweight properties [1]. These structural components are often assembled in conjunction with metal parts using mechanically fastened joints resulting in hybrid metal-composite joints which determine some challenging problems for mechanical engineers. Poor designed hybrid joints are not only a source of failure, but could lead to a reduction in durability and reliability of the whole aerospace structure. To avoid the expensive and time consuming experiments, the numerical method correlated with tests, represents an efficient solution for increasing the design efficiency. The influence of the temperature on the linear elastic behavior and axial stiffness of the single lap, single-bolt metal-composite joints has been studied by Z. Kapidžić et al. [2], E. Chaves et al. [3] and N. PARKES [4]. Due to existing manufacturing and drilling tolerances, the clearances do exist in assembly process and these clearances can affect the axial stiffness of

the joint as it has been reported in the literature [5-7]. Thermal expansion can modify these clearances and thus modifying the axial stiffness. Moreover, the drilling process affects the sensitivity of the material to local stress concentrations around the hole and thermal loading can increase this material sensitivity. The aim of this study is to experimentally investigate the influence of the temperature variations on the linear elastic response of the single-lap, single-bolt, metal-composite joints.

2. PROBLEM DESCRIPTION

The joint geometry proposed for this study is a standard configuration related to the characterization of mechanically fastened composite joints, MIL-HDBK-17, [8], [9] and ASTM D 5961/D 5961M-96, [10]. In these standards it states that single lap joint configuration is more representative than double lap ones for the most critical bolted joints configuration in space applications. The specimen geometry is shown in Fig. 1. The joint geometry is based on the ASTM standard D 5961/D 5961 M-96, [10]. The geometric ratios, w/d = 8.8, e/d = 2, d/t = 1.25, were designed to induce bearing failure. For the hybrid metal-composite joint, the composite plate is made from carbon fibre/venyl-ester epoxy prepregs, a high-modulus material and it was manufactured by Fibertech Italy. The prepregs's carbon fiber is Toray T 300 [11] with the resin Derakane Momentum 411-350 [12] venyl-ester epoxy having $V_f = 0.32$ carbon fiber volume fraction. The lay-up is one quasi-symetric with stacking sequence [0/90/0/90/0/90], including six layers arranged starting from bottom to top surfaces in the Z direction. The ply nominal thickness is 0.5 mm, yielding a total laminate thickness of 3 mm when cured. The metal counterpart plate is made from alluminum alloy AA 7075 T6 [13], having 4 mm thickness. The bolts used were stailess steel A2-70 [13] fasteners with nominal diameter of 5 mm. The same stainless steel material was used for nuts and washers.

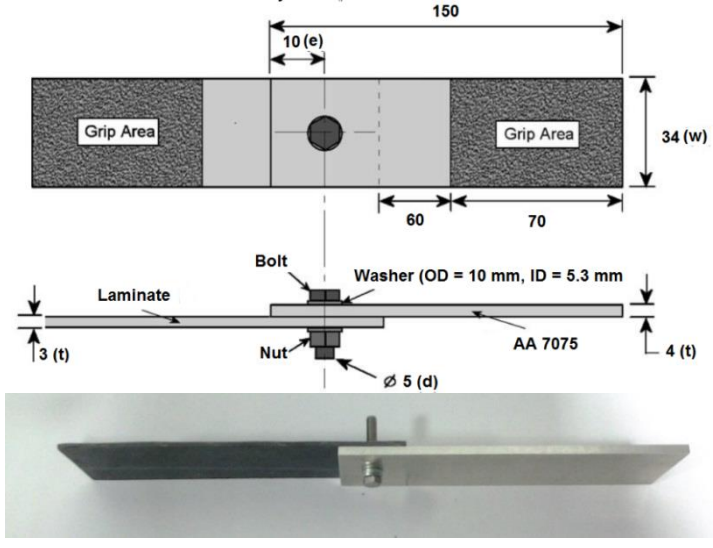

Fig. 1 Specimen geometry, all dimensions in mm

The experimental tests involved over 5 specimens loaded in elastic range of the composite plate for two values of temperature $T_1 = -50\ ^oC$, and $T_2 = +50\ ^oC$, in order to investigate the thermal effects on the axial stiffness of the joint and the 3D stress field around the hole boundary. In the tensile tests, the bolts were installed with 0.5 Nm torque level.

3. FINITE ELEMENT MODEL DEVELOPMENT

A tridimensional finite element model, using linear eight nodes brick elements, was developed in commercial software MSC Patran for the joint geometry, shown in Fig. 2. Each separate part was meshed: metal and composite plates, two washers and a combined bolt-nut part. The plates were modelled with high radial mesh density around the hole, under the washers where high strain gradients exist.

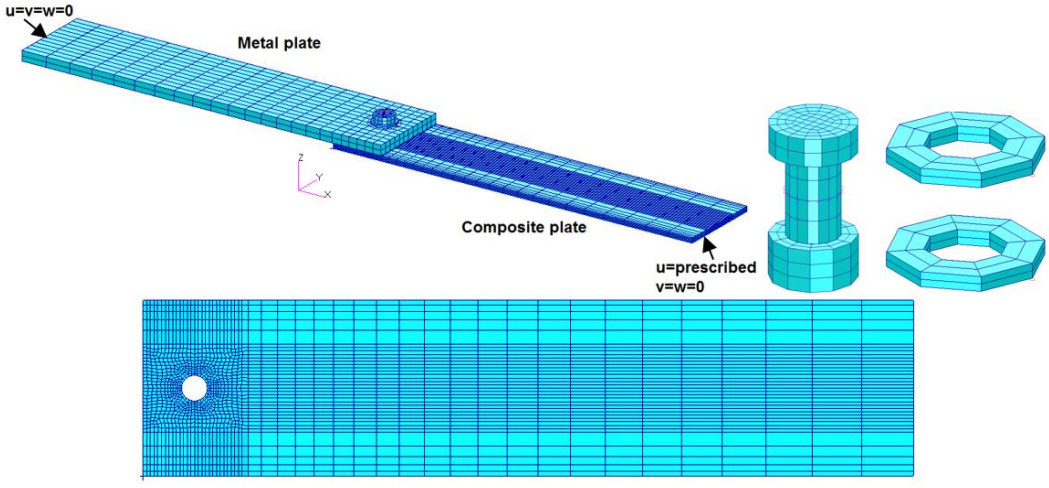

Fig. 2 Finite element model with boundary conditions

Regarding the boundary conditions, the left side end of the metal plate is clamped and the right side end of the composite plate is allowed to move only on X axis, where a prescribed of 3 mm/min displacement rate is imposed for simulating the stationary loading condition. In order to avoid rigid body motions, light springs were attached to the components not fully constrained, such as the bolt, washers and laminate plate. For simulating the bolt preload due to the torque level, a 330 N axial force was applied in the bolt shank using Bolt Preload Module in Patran.

The unidirectional elastic properties were obtained using ASTM [14], [15] standard tests on the unidirectional laminated coupons and they are presented in Table 1. The laminated plate is modelled with continuum solid-shell special elements available in Nastran 2011. These special solid elements have shell bending properties and only one integrating point per element. The finite element model has six elements per laminate thickness, with one solid-shell element per each ply, thus, the stress in each ply can be determined and the correct bending-twisting coupling is obtained.

The metal counter plate, the bolt, nut and washers were modelled using isotropic materials properties with elastic properties: $E_{AA\ 7075}$ = 71000 MPa, $\upsilon_{AA\ 7075}$ = 0.33, E_{steel} = 206000 MPa, υ_{steel} = 0.36.

Table 1. Unidirectional lamina elastic properties for laminate plate

E_{11} (MPa)	E_{22} (MPa)	E_{33} (MPa)	G_{12} (MPa)	G_{13} (MPa)	G_{23} (MPa)	ν_{12}	ν_{13}	ν_{23}
34433	3610	3610	2421	2421	1561	0.36	0.36	0.45

The thermal expansion coefficients for the metallic parts are taken from standard [13] and these are: $\alpha_{aluminum}$= 24 (10^{-6}/ ^{o}C), α_{steel}= 18 (10^{-6}/ ^{o}C). Regarding the thermal expansion coefficient of the composite plate, it has been used a microanalysis method to calculate this

coefficient at lamina level using the thermal coefficients of the fibers and matrix. According to [11] and [12] we have α_{fiber}= - 0.41 (10^{-6}/ ^{o}C), α_{matrix}= 40 (10^{-6}/ ^{o}C). Using these values and equation (1) we can obtain:

$$\alpha_{11}=\frac{E_{fiber}\cdot V_f\cdot\alpha_{fiber}+E_{matrix}\cdot(1-V_f)\cdot\alpha_{matrix}}{E_{11}} = 2\ (10^{-6}/\ ^{o}C) \quad (1)$$

$$\alpha_{22} = \alpha_{33} = 44\ (10^{-6}/\ ^{o}C), \text{ transversal isotropy hypothesis, [12]} \quad (2)$$

In the 3D model, the contact between the bolt and the hole surface is achieved by direct method of the constraints explained in the following. The method requires the definition of contact bodies, bodies that can interact. The bodies in contact may be whole physical bodies (laminated plates, bolt, washers) but it has been shown [16] that it is more efficient to consider sets of elements of these physical bodies in contact, as shown in Fig. 3, because the number of checks for contact between bodies at each iteration of the solution is reduced.

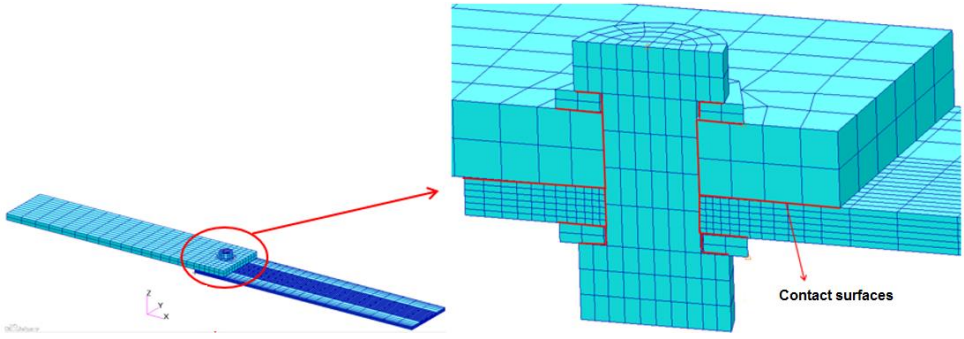

Fig. 3. Contact bodies in 3D model

A specific tolerance is used to determine if a node penetrates the nearest segment and then it is considered to be in contact with that segment; if so, it is moved to the segment and constrained to stay on it. If the node penetrates the tolerated contact area, the solution is resumed and a new node position is calculated by checking if it is in the contact tolerated area. If the tolerance is too small then the iteration time of the solution and the determination of the node position in the tolerated zone will be very long and considerable hardware resources will be required, but too big tolerance will lead to a premature and unrealistic determination of the contact between two bodies. The default contact tolerance value in PATRAN is the twentieth part of the smallest side of the smallest element. In PATRAN, there is the possibility of defining contact as "single-sided" or "double-sided", the contact between the bodies is made in one sense or in both senses and the order in which the two bodies are defined in contact is important. In the present paper, only the "single-sided" contact is used, since the "double-sided" variant can lead to cracks at the contact interface, and the joining component with the finer (stiffer) mesh has to be defined the first (slave) in the process of defining the contact; the component with a coarser mesh must be defined the second (master). This order for defining the bodies in contact has a direct implication on the restrictions imposed on the FEM model of the joint. Another step in defining nonlinear contact phenomena is the choice between the analytical contact and the discreet contact, which will be briefly described below. When a node on a solid reaches the contact segment on the other solid, the node is constraint on this segment along the normal to this segment. In the case of discrete contact for normal detection, the linear representation with the finite elements of the contact surface is used which leads to the calculation of the normal of each element. If the surface is not planar, when the node touches the contact segment on the

surface of the other solid in contact, being in the tolerated contact area, it is shifted and constrained on the contact segment, making it possible for the moving process and constraint; the surface having a curve, the node is blocked between 2 differently normal elements due to the discontinuity of the normal elements. This impediment has an adverse effect on the quality of the results as observed by McCarthy et al. [16] in their work on single bolt joint, single shear of composite materials. In the case of analytical contact, a smooth Coons surface is constructed through the nodes of the solid contact segment, and then this analytical surface is used to calculate the continuous normal at the contact surface between the two solid elements, thus solving the problem of node blocking due to the discontinuity of normal vector to contact surface between the bodies. This method leads to a better representation of the geometry of the joint, especially its deformation and the accuracy of the numerical results is far superior to the technique of discrete contact [16].

4. RESULTS AND DISCUSSION

- Model Validation

In this section, the results from the tests are compared to the simulation results of the three-dimensional finite element model described in the previous chapter. Strains at selected points on the top and bottom surfaces of the laminated plate are used to check the accuracy of the finite element model. The joints were strain gauged and loaded in traction to a level that prevents any damage of the composite plate (2 kN). Fig.4 presents the locations of the strain gauges with 3 mm length; all gauges are aligned with the loading direction and located on the top surface of the laminate plate, except the gauge number 2 which is located in the shear plane on the bottom surface. The numerical and experimental results for strains are shown in Table 2.

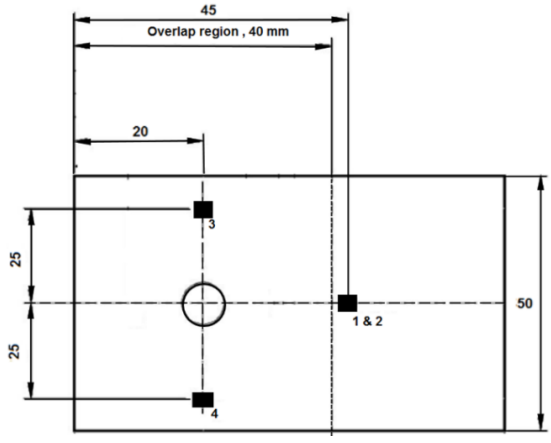

Fig. 4 Strain gauge locations, all dimensions in mm

Table 2. Experimental and numerical strains at 2 kN applied load, T=+50 ^{0}C

Gauge number	Experimental strain (μm/m)	Numerical strain (μm/m)
1	-1.8	-1.5
2	760	633
3	-400	-346
4	-353	-315

From the Table 2 it is clearly seen that strain gauges 1 and 2 indicate a joint bending despite the fact that the loading is a tensile as it is presented in Fig. 5. The strain readings for gauges number 3 and 4 are quite different indicating a twisting effect of the joint along the longitudinal axis which is the loading axis as can be seen in Fig.6. Fig. 6 presents the displacements on the Z axis of the points located on two curves C 1 and C 2 (originating in the right end of the plate) on the two sides in the median plane of the composite plate. As can be seen from Fig. 6, the points on the curve C 2 having $10 < X < 75$ mm have Z-axis displacements greater than the corresponding points on the curve C 1, which means a turn of the plate from the longitudinal axis of symmetry of the plate. The points located in the second half of the plate, towards the right end, have zero displacement on the Z-axis due to the clamping of the plate between the test machine's grips. As a conclusion from Table 2, it can be considered that the model predicts the linear behavior of the joint quite accurate and can be used in the following temperature parametric study for the linear response of the hybrid metal-composite joint.

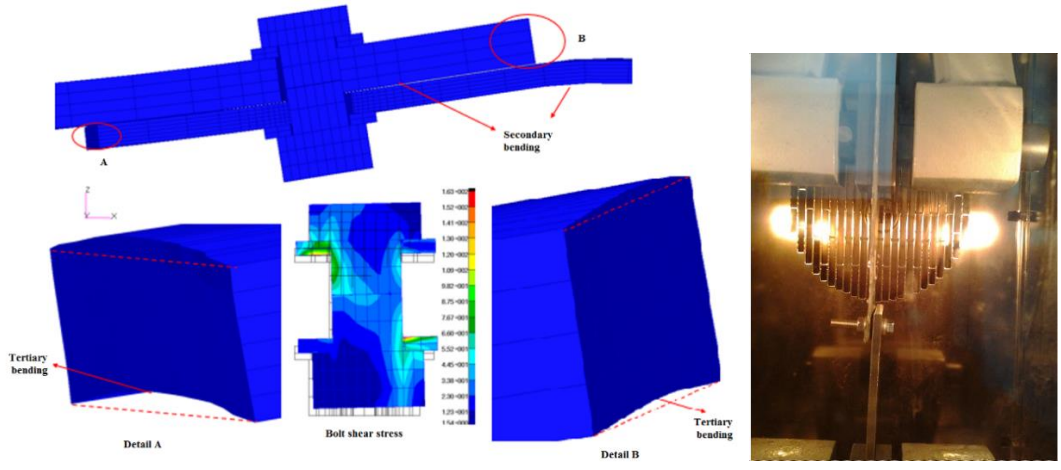

Fig. 5 Joint secondary bending

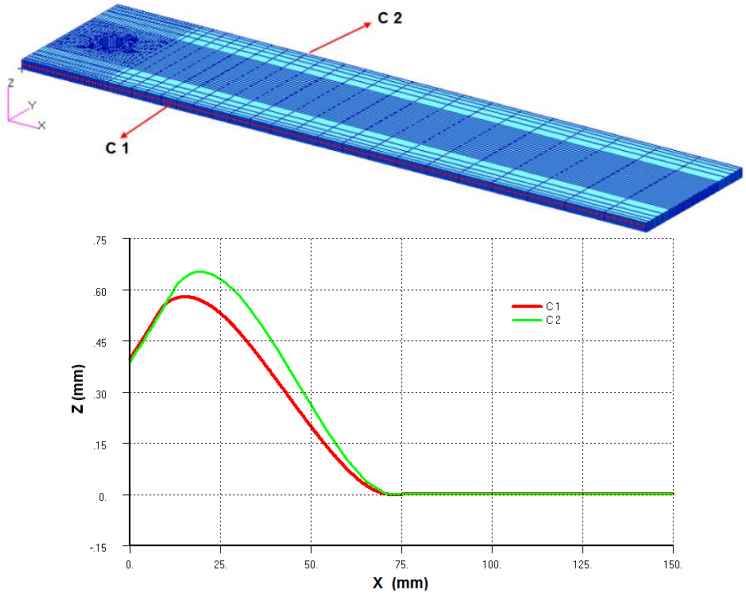

Fig. 6 Joint twisting effect

- Joint stiffness

From the experimental results it was observed that the load-displacement curves are approximately linear between the applied forces 0.9-2.5 kN in the experiment and 0.9-3 kN in the analysis for temperature T = +50 ^{0}C, but 0.7-2.3 kN in the experiment and 1.2-3 kN in the numerical simulation for temperature T = - 50 ^{0}C, so the stiffness of the joint is measured for these ranges. The joint load was obtained directly from the testing machine, and the displacement was measured with an optical extensometer. The load-displacement curves for the two temperature values are presented in Figs. 7 and 8.

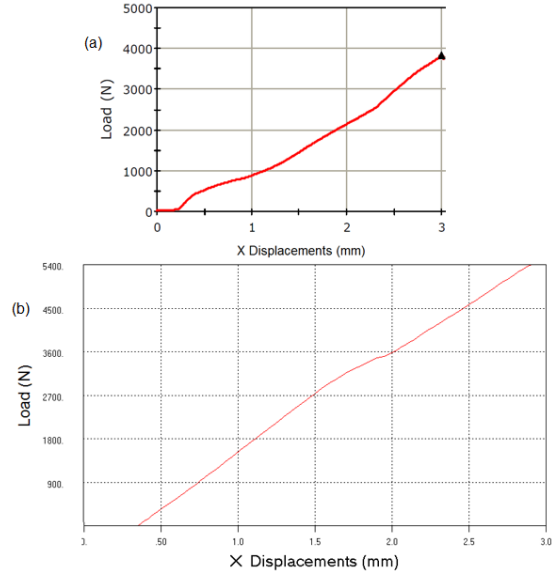

Fig. 7 Load-displacement curve for T = +50^{0}C, (a) - experiment, (b)-simulation

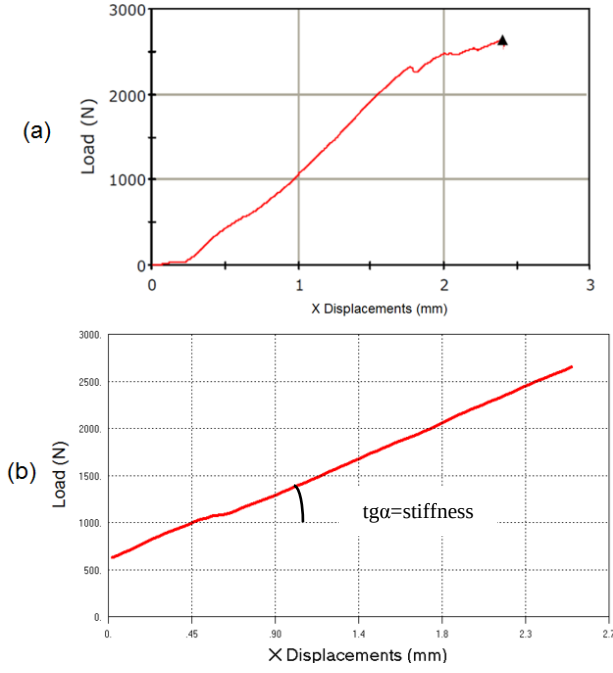

Fig. 8 Load-displacement curve for T = -50^{0}C, (a) - experiment, (b)-simulation

The first nonlinear segments on the curves from Figs. 7 and 8 are explained by the friction effects between the plates.

For low level of the applied load, the forces are transmitted through the friction and the plates do not move relatively to each other, so the shank of the bolt do not bear the hole surface due to the initial clearance fit in the joint.

The joint under investigation has a close tolerance clearance equal to 48 μm according to f 7 H 10 standard fit tolerances.

As long as $F > \mu P$, where F is the applied joint load, $\mu=0.235$ is the frictional coefficient between aluminum AA 7075 and CFRP plates as Schon [17] measured experimentally and P=330 N is the plates clamping force due to preload, the friction is overcome and the bolt shank bears the hole surface.

From now on, the joint is elastically deformed; the axial stiffness is fully developed and can be determined. Figs. 7 and 8 are presented only for describing linear behavior of the hybrid metal-composite bolted joints, despite that in Fig. 8 some nonlinearity is observed at the end of the curve due to some damage initiation in the laminate plate, but this phenomenon will be ignored in this paper. The experimental and numerical axial stiffness, calculated as the slope of the approximately linear portions of the load-displacement curves, are presented in Table 3.

Table 3. Experimental and numerical results for axial stiffness

Stiffness (kN/mm)		Temperature (^{0}C)
Experiment	Simulation	
1.12	1.44	+50
0.74	0.95	-50

From Table 3 it can be observed that the temperature stiffen the hybrid metal-composite joint both in the experiment and simulation results.

The reason for the joint stiffening is that the material thermal expansion reduces the joint clearance and thus increasing the joint local stiffness of the overlap portion of the plates. As expected the FEM model joint is stiffer than the experimental one due to the mesh size effect which cannot be completely eliminated.

- 3D stress field around the hole

The effects of the temperature on the 3D stress field around the hole in the laminate plate are presented in this section.

The radial (σ_R) and tangential (σ_θ) stresses in each ply are plotted in a cylinder coordinate system (R, θ, Z) with the origin located in the hole center, in order to better understand the influence of the temperature on the stress field.

Due to the fact that the approximation linear region of the load-displacement curve for both temperature values ranges between 0.9 and 3 kN applied load, the 3D stress field will be plotted for 1.5 kN and 2.5 kN of this load.

The influence of the temperature on the tangential and radial stresses on the surface hole of laminate plate is plotted in Figs. 9-14 with a diagram including the variation of the stress through the thickness of the plate in the most critical areas. In Figs. 9-14, the total (mechanical and thermal) stresses are plotted on the hole surface as a whole overview of the 3D stress field.

The stress field in laminate plate is important because the joint failure is established due to the damage initiation in the composite plate.

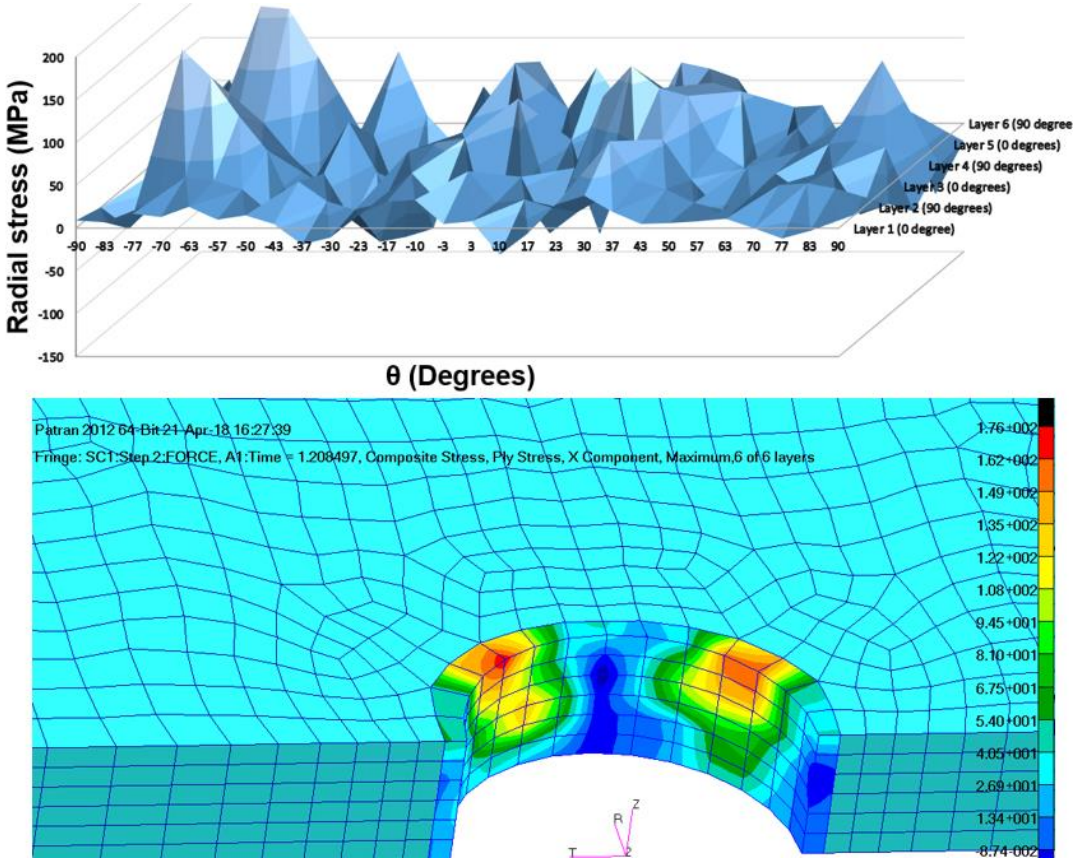

Fig. 9 Radial stress on hole surface, F=1.5 kN, T=+50 ^{0}C

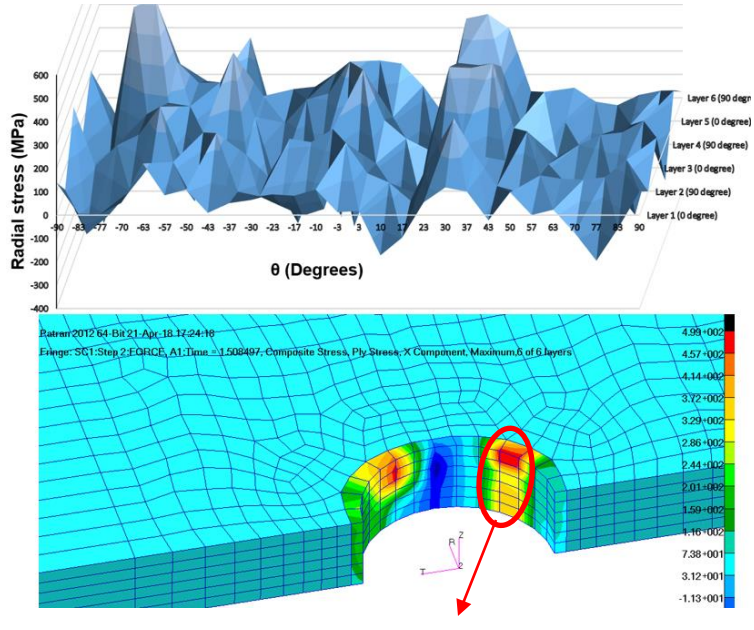

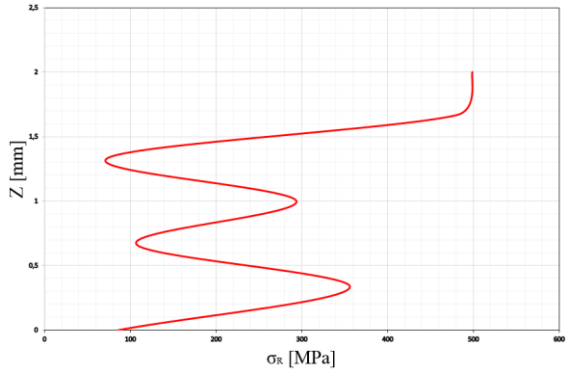

Fig. 10 Radial stress on hole surface, F=2.5 kN, T=+50 ^{0}C

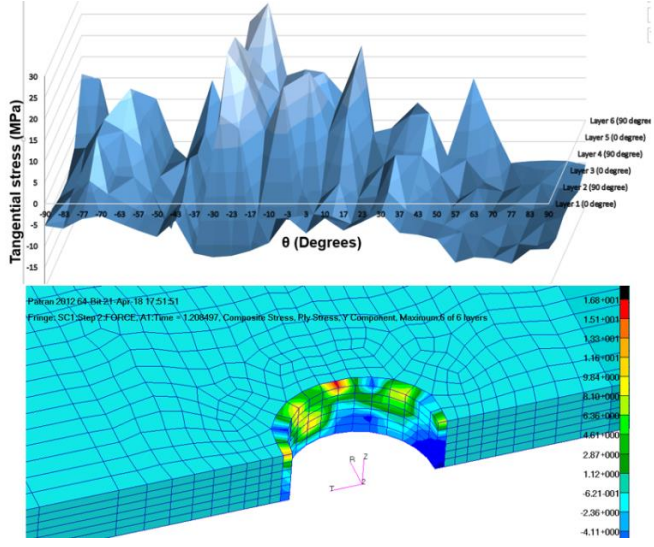

Fig. 11 Tangential stress on hole surface, F=1.5 kN, T=+50 ^{0}C

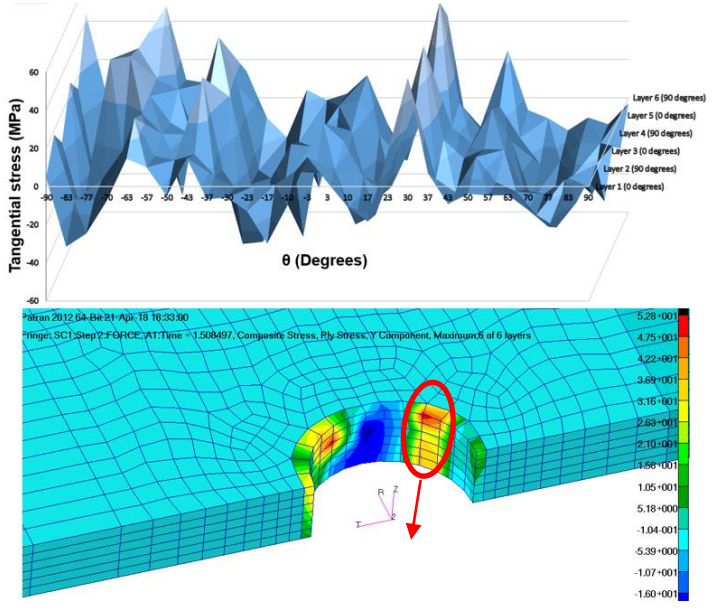

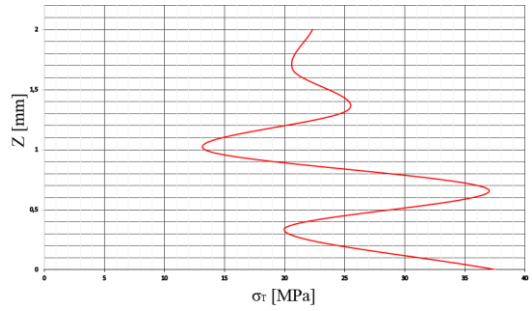

Fig. 12 Tangential stress on hole surface, F=2.5 kN, T=+50 ^{0}C

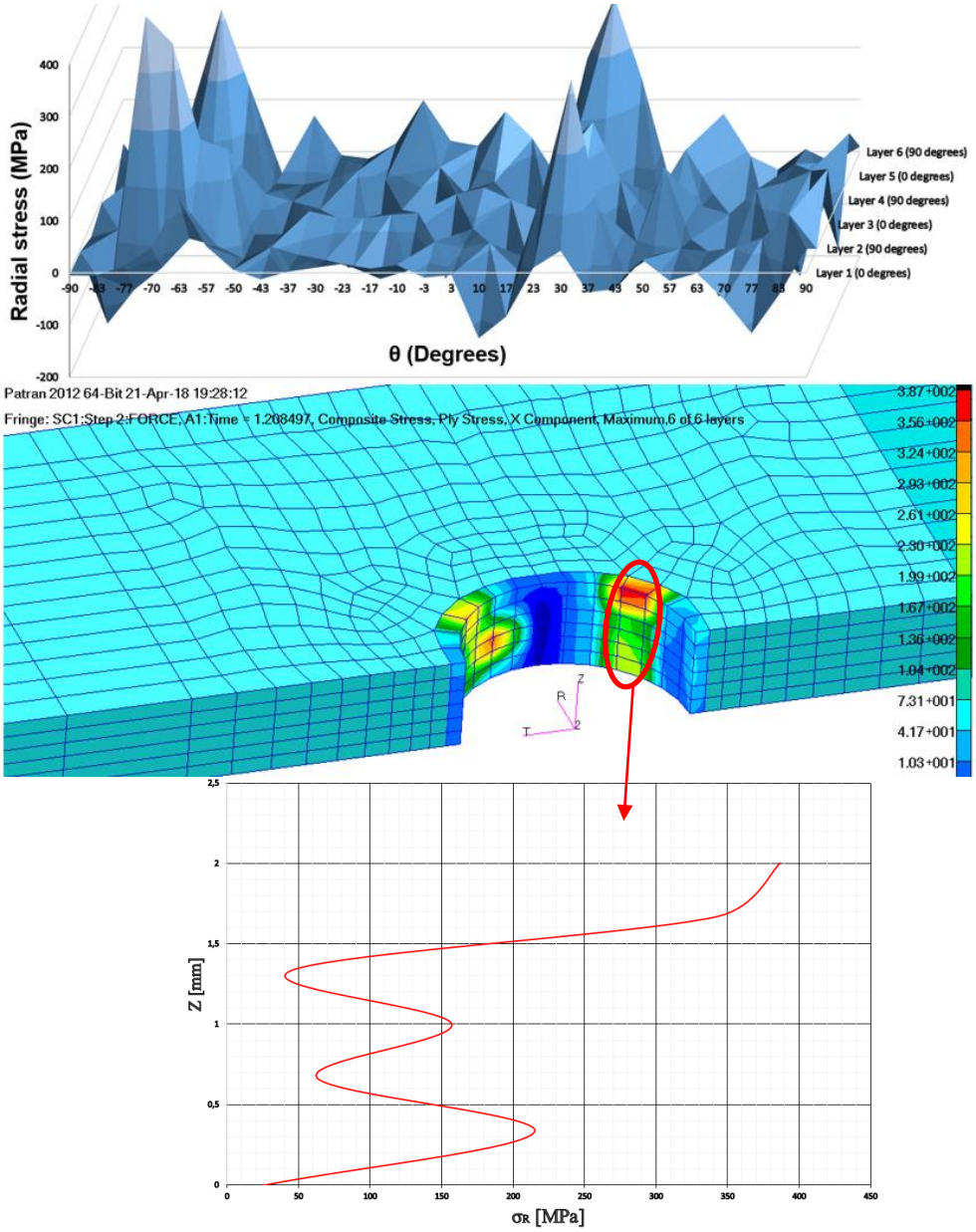

Fig. 13 Radial stress on hole surface, F=1.5 kN, T=-50 ^{0}C

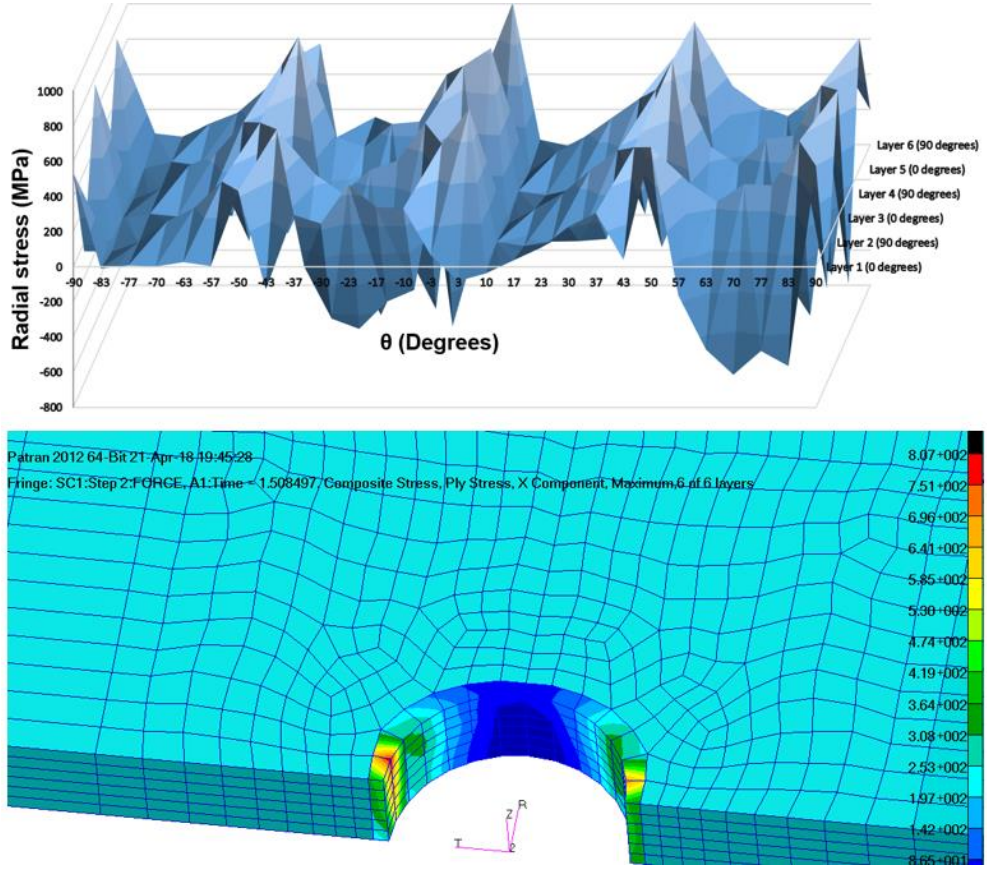

Fig. 14 Radial stress on hole surface, F=2.5 kN, T=-50 ^{0}C

Table 4. Temperature effects on the 3D stress field around the hole

Temperature (^{o}C)	Max. radial stress (MPa)	Max. tangential stress (MPa)	Load (kN)
50	176	16.8	1.5
-50	387	42.5	
50	500	52.8	2.5
-50	807	110	

In order to make the influence of temperature on the 3D stress field around the hole easier to understand, the results shown in the Figs. 9-14 are summarized in Table 4. From the Table 4 and Fig. 9-14, it can be concluded that the temperature loading reduces the stress field on the hole surface due to the fact that initial clearance between the bolt shank and the surface hole is consumed through free dilatation of the composite plate which increases the contact area between the both parts, and thus reducing the contact stress and the radial stress on the hole surface. As an example, a temperature increase of 100 ^{o}C, at 1.5 kN constant load, the peak radial stress is almost half reduced from 387 MPa down to 176 MPa, which represents the thermal expansion effect only. For 2.5 kN load case, this thermal effect is reduced due to a higher mechanical loading, as can be seen from Table 4. On the other hand mechanical loading increases the radial and tangential stresses as can be seen from the Table

4 as it was expected. The radial stresses on the hole surface are responsible of the joint bearing failure mode, while the tangential stresses in the points corresponding to $\theta=0^o$ and 180^o are responsible of the joint net-section failure mode, but stress influence is beyond the scope of the paper. The non-uniform contact stress distribution on the hole surface of the laminate plate is justified by the complex 3D deformation as shown in Fig. 5 due to the superposition of the bending and twisting effects.

5. CONCLUSIONS

In this paper a detailed 3D FEM model with continuum elements is developed for a single lap, single bolt, composite-aluminum hybrid joint. The aim of this study was to experimentally investigate the influence of the temperature on the linear elastic response of the metal-composite joints. The model accounted for all mechanism that were expected to influence the joint stiffness and the 3D stress field around the hole, including fastener preload, member plates friction, bolt–hole clearance, nonlinear kinematics and temperature. The numerical model was calibrated and validated using surface strain readings before the temperature parametric study. The FEM model was found to be quite accurate in term of the load–displacement curves on linear range of the mechanical behavior of the joint.

The main authors contribution represents the study of thermal effects on the axial joint stiffness and 3D stress field around the hole which was described in chapter 4. It was concluded that the temperature stiffens the hybrid metal-composite joint both in the experiment and simulation results, as it can be seen from Table 3 due to the fact that thermal expansion reduces the initial clearance in the joint. Another observation was that the FEM model is stiffer than the experimental one due to the mesh size effect which cannot be completely reduced. The clearance in the joint was found to be the most important parameter affected by the temperature variations which can influence the joint stiffness and the stress field around the hole, if member plates with different thermal expansion coefficients are used. Regarding the thermal effects on the stresses around the hole it was shown that the temperature loading reduces the stresses due to the fact that 48 μm initial clearance between the bolt shank and the surface hole is consumed through free dilatation of the composite plate. The non-uniform contact stress distribution on the hole surface of the laminate plate is justified by the complex 3D deformation, as shown in Fig. 5 due to the superposition of the bending and twisting effects.

REFERENCES

[1] Y. Xiao, T. Ishikawa, Bearing strength and failure behavior of bolted composite joints (part II: modeling and simulation), *Composites Science and Technology*, **65**, pp. 1032–1043, 2005.

[2] Z. Kapidžić, H. Ansell, J. Schön, K. Simonsson, Fatigue bearing failure of CFRP composite in biaxial loaded bolted joints at elevated temperature, *Compos. Struct.* **127**, pp. 298–307, 2015.

[3] C. E. Chaves, D. J. Inforzato, F. F. Feernandez, Principles of Mechanical Fastening in Structural Applications, *Joining of Polymer-Metal Hybrid Structures: Principles and Application*, **1**, pp. 147-164, 2018.

[4] P. N. Parkes, R. Butler, D. P. Almond, *Fatigue of metalcomposite joints with penetrative reinforcement*, Proceedings of 54th AIAA/ASME/ASCE/AHS/ASC Structures, Structural Dynamics and Materials Conference, pp. 1−9, 2013.

[5] M. A. McCarthy, V. P. Lawlor, W. F. Stanley, An experimental study of bolt-hole clearance effects in single-lap, multi bolt composite joints, *J. Compos. Mater.* **39**, pp. 799–825, 2005.

[6] M. A. McCarthy, C. T. McCarthy, G. S. Padhi, A simple method for determining the effects of bolt-hole clearance on load distribution in single-column multi-bolt composite joints, *Compos. Struct.* **73**, pp. 78–87, 2006.

[7] B. Egan, C. T. McCarthy, M. A. McCarthy, R. M. Frizzell, Stress analysis of single-bolt, single-lap, countersunk composite joints with variable bolt-hole clearance, *Compos. Struct.,* **94**, pp. 1038–1051, 2012.
[8] * * * DODSSP, *Polymer matrix composites, MIL-HDBK-17, DODSSP*, Naval Publications and Forms Center, Standardization Documents Order Desk, Philadelphia, PA [19111-5094].
[9] P. Shyprykevich, Characterization of bolted joint behaviour: MILHDBK- 17 accomplishments at standardization, *J. Composites Technol Res.*, **17**(3), pp: 260–70, 1995.
[10] * * *ASTM standard D 5961/D 5961M-96, Standard Test Method for Bearing Response of Polymer Matrix Composite Laminates, 1996.
[11] * * * Torayca T300 Technical Data Sheet No. CFA-001, Toray Carbon Fibers America Inc, www.torayusa.com
[12] * * * Derakane Momentum 411-350 Epoxy Venyl Ester Resin, Technical Data Sheet No. 1701 V3 F2, Ashland Inc, www.ashland.com
[13] * * * MMPDS-05, Metallic Materials Properties development and Standardization, Federal Aviation Administration, 2010
[14] * * * ASTM D 3039, Standard Test Method for Tensile Properties of Polymer Matrix Composite Materials, ASTM International.
[15] * * * ASTM D 5379, Standard Test Method for Shear Propeties of Composite Materials by the V-Notched Beam Method, ASTM International.
[16] M. A. McCarthy, C. T. McCarthy, V. P. Lawlor, W. F. Stanley, *Three-dimensional finite element analysis of single-bolt, single-lap composite bolted joints: part I - model development and validation*, November 2004.
[17] J. Schon Coefficient of friction for aluminum in contact with a carbon fiber epoxy composite, *Tribol Int*; **37**(5), pp: 395–404, 2004.